Treatment of tooth fracture by medium energy CO_2 laser and DP-bioactive glass paste: Thermal behavior and phase transformation of human tooth enamel and dentin after irradiation by CO_2 laser

C. P. LIN, B. S. LEE, S. H. KOK, W. H. LAN
Graduated Institute of Dental Sciences, College of Medicine, National Taiwan University, Taipei, Taiwan

Y. C. TSENG, F. H. LIN*
Institute of Biomedical Engineering, College of Engineering and Medicine, National Taiwan University, Taipei, Taiwan
E-mail: double@ha.mc.ntu.edu.tw

Acute trauma or trauma associated with occlusal disharmony can produce tooth crack or fracture. Although several methods are proposed to treat the defect, however, the prognosis is generally poor. If the fusion of a tooth fracture by laser is possible it will offer an alternative to extraction or at least serve as an adjunctive treatment in the reconstruction. The responses of soft tissues to lasers of different wavelengths are fairly well known, but the reactions of hard tissues are still to be understood. The purpose of this research was to study the feasibility of using a medium energy continuous-wave CO_2 laser and a low melting-point bioactive glass to fuse or bridge tooth fractures. The present report is focused on the first part of the research, the analysis of changes in laser-irradiated human tooth enamel/dentin by means of X-ray diffractometer (XRD), Fourier-transforming infrared spectroscopy (FTIR), differential thermal analysis/thermogravimetric analysis (DTA/TGA), and scanning electron microscopy (SEM). After CO_2 laser irradiation, there were no marked changes in the X-ray diffraction pattern of the enamel when compared to that before laser treatment. However, a small peak belonging to α-TCP appeared at the position of $2\theta = 30.78\,^{\circ}C$. After being treated with CO_2 laser, the dentin showed much sharper peaks on the diffraction patterns because of grain growth and better crystallinity. α-TCP and β-TCP were identified after laser treatment. In the FTIR analysis, an HPO_4^{-2} absorption band was noted before laser treatment disappeared after the irradiation. No significant change in the absorption band of HPO_4^{-2} was found on the FTIR curves of enamel after laser treatment. The results of DTA/TGA indicated that loss of water and organic materials occurred in both enamel and dentin after laser treatment. Under SEM, melting and resolidification occurred in both enamel and dentin by medium energy of CO_2 laser. This implies that using a continuous-wave CO_2 laser of medium energy density to fuse a low melting-point bioactive glass to the enamel/dentin is possible. We believe these phase changes and thermal data can make a useful guide for future studies on the thermal interaction and bridging mechanism between the bioactive glass and enamel/dentin under CO_2 laser irradiation.

1. Introduction

Fracture of teeth, including cracked tooth syndrome, is a common clinical problem. Subclinical microfracture of the enamel is also frequently seen. However, when the fracture is more extensive and involves the dentin, it may become catastrophic, leading to a major loss of dental hard tissues and the exposure of deep dentin or pulp. Such an occasion constitutes a dental emergency, and requires major dental surgical intervention, where the vitality of the tooth is at risk [1–3].

*Author to whom all correspondence should be addressed.

Acute trauma and trauma associated with occlusal disharmony or extreme clenching and gritting can produce crown and/or root fracture. The defect can be a complete fracture, but may at times extend through only part of the root or crown. Root fracture frequently necessitates dental extraction. Although techniques for repairing dental fractures have been proposed, such as filling the fracture lines or zones by amalgam, cyanoacrylate, glass ionomer, or the Gluma bonding system [4–6], the long-term prognosis remains questionable. If the fusion of a tooth fracture by laser is possible, it will offer an alternative to extraction or at least serve as an adjunctive treatment in the reconstruction. Although investigations about the effects of lasers on the enamel/dentin are numerous [7–9], only limited effort has been devoted to the use of lasers to fuse dental cracks or fractures, or to melt biomaterials to the fracture spaces.

Stewart *et al*. [7] reported a technique of using a CO_2 laser to melt synthetic hydroxyapatite onto the enamel by combining hydroxyapatite with a low fusing eutectic. Arakawa *et al*. [9] induced root fractures, irradiated them by Nd : YAG laser with air/water surface cooling, and then filled the fractures with a paste of tricalcium phosphate. The results revealed that fusion did not occur under such conditions because of tissue dehydration and subsequent enlargement of the gap of fracture [8, 10].

In a series of our study, the authors try to use a continuous-wave CO_2 laser of medium energy density to fuse a low melting-point bioactive glass to the enamel/dentin. The bioactive glass has a strong absorption band at the wavelength of 10.6 μm, and is expected to be melted and fused with the dental hard tissues after exposure to CO_2 laser. The study was divided into three parts: 1. The compositional and structural changes in tooth enamel and dentin after CO_2 laser irradiation; 2. The phase transformation and recrystallization of the low melting-point bioactive glass after treatment; 3. The thermal interaction and bridging mechanism between the bioactive glass and enamel/dentin subjected to CO_2 laser.

Although phase changes in the laser-irradiated enamel/dentin have been expected, no studies have been reported to confirm the appearance of new compounds or compositional and structural changes in dental hard tissues irradiated by lasers [11, 12]. Therefore, the present report is focused on the first part of the study, to analyze the changes occurred in the laser-irradiated human tooth enamel/dentin by means of X-ray diffraction (XRD), Fourier-transforming infrared spectroscopy (FTIR), differential thermal analysis/thermogravimetric analysis (DTA/TGA), and scanning electron microscopy (SEM).

2. Materials and methods

2.1. Specimen preparation

Extracted human molars were used in the study. Crowns with caries, restoration and fractures were excluded. The remaining soft tissue was removed from the tooth surface with a dental scaler (Sonicflex 2000, KaVo Co., Biberbach, Germany). All teeth were then stored in 4 °C distilled water containing 0.2% thymol to inhibit microbial growth until use.

The crown was amputated fully hydrated from each tooth, by means of a slow speed saw (Isomet; 10.2 cm × 0.3 mm, arbor size 1/2 inch, series 15HC diamond; Buehler Ltd, Lake Bluff, IL). Enamel or dentin block with a surface area of $4 \times 3\ mm^2$ was obtained and wet polished to 600-grit (silicon carbide, SiC). On the other hand, the fragments of enamel/dentin were removed using a plain-cut tungsten carbide fissure bur at high speed under water spray, and then were pulverized into powder of an average particle size of 106 μm. The enamel/dentin powder was prepared for XRD, FTIR and DT/TG analysis, and the enamel/dentin blocks were prepared for SEM examination.

2.2. Laser treatment

The LUXAR LX-20 CO_2 laser (Luxar Corp., Bothell, WA) was operated at 5 W power setting, using a focused (2 mm from target surface) continuous waveform beam delivered through a 0.8 mm diameter ceramic tip. The efficiency of the delivery of beam energy was 86% as determined by the manufacturer of the model. The time for each exposure was 5 s and the total irradiation time was 1 m. Thus the calculated energy density was 2500 J/cm^2. Before irradiation, powder form specimen was compacted into a disk (3 mm in diameter and 1 mm in thickness) with a hydraulic force of 50 kg/cm^2, to prevent the powder from rising up or fluttering in the air during laser beam sputtering.

2.3. X-ray diffraction (XRD)

The crystalline phases of the specimens before and after laser irradiation were determined by a Rigaku X-ray powder diffractometer (Rigaku Denki Co. Ltd, Tokyo, Japan) with CuKα radiation and Ni filter. The scanning range was from 10° to 60° with a scanning speed of 4°/min. To determine the contents of different phases, relative intensities of the characteristic peaks of each phase were used.

2.4. Fourier-transforming infrared spectroscopy (FTIR)

The phase transformation after laser treatment was studied with FTIR. The FTIR spectra were recorded using KBr pellets (1 mg sample per 300 mg KBr) on a Jasco FTIR grating instrument (FTIR–300E, Jasco International Co. Ltd, Tokyo, Japan) with slow scan and normal slit width. The wavelength used was in the range of 4000–400 cm^{-1} to evaluate the functional groups in the specimens.

2.5. Differential thermal analysis/thermogravimetric analysis (DTA/TGA)

Thermal behavior under laser irradiation was recorded by a TA/SDT2960 (TA Instruments Inc., New Castle, DE) for DTA/TGA. The scanning temperature was from room temperature up to 1500 °C with a heating rate of 20 °C/min and N_2 flow rate of 90 ml/min. The total weight of the specimen for each thermal analysis was 40 mg, using Al_2O_3 as the reference powder.

2.6. Scanning electron microscopy (SEM)

The morphology and microstructure of the specimens were observed under a scanning electron microscope. After laser treatment, the specimens were immersed in 2.5% cold glutaraldehyde in 0.1 mol/L cacodylate buffer at pH 7.4 for 8 h. Subsequent to the initial fixation, specimens were rinsed in buffer and postfixed with 1% osmium tetraoxide for 4 h. All specimens were then serially dehydrated in graded ethanol solutions (50, 60, 70, 80, 90, 95, 100% ethanol) at 45-min intervals, and critical point-dried by the CO_2 method of Anderson [13]. Finally, all specimens were mounted on aluminum stubs and sputter-coated with ~ 20 nm of gold/palladium before being examined under a Hitachi SEM (Model S-800, Tokyo, Japan).

3. Results

3.1. XRD analysis

When compared to the standard Joint Committee on Powder Diffraction Standards (JCPD) card, the XRD diffraction pattern of the enamel powder before CO_2 laser irradiation was identified as hydroxyapatite and the peaks were in agreement with those in the standard hydroxyapatite diffraction pattern (Fig. 1a). Three reflected peaks of (0 0 2), (1 1 2) and (4 1 2) in the enamel were much stronger than those in the standard pattern because of the preferred orientation in these directions. After exposure to the CO_2 laser, there were no significant differences in the XRD pattern of enamel as compared with that before laser treatment. However, a small peak belonging to α-TCP appeared at the position of $2\theta = 30.78°$ (Fig. 1b).

The XRD pattern of the dentin powder was identified as a nonstoichiometric hydroxyapatite structure (Fig. 2a). There was a broad peak at the position of $2\theta = 30°$–$50°$ because the particle size of the hydroxyapatite in dentin was very small, only about 30–60 nm. The fact that OH^- groups of hydroxyapatite in dentin are frequently replaced by CO_3^{-2}, F^- and Cl^- also contribute to the broad peak in these patterns [14]. After CO_2 laser treatment, all peaks in the XRD patterns of dentin turned sharper (Fig. 2b). Furthermore, four peaks other than hydroxyapatite could be traced at the positions of $2\theta = 30.78°/34.21°$ and $32.47°/33.05°$ which were identified as α-TCP and β-TCP, respectively.

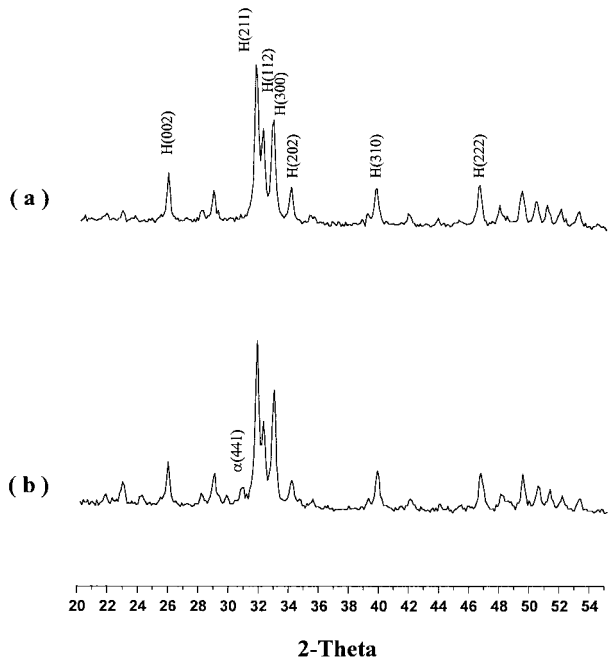

Figure 1 X-ray powder diffraction patterns of the enamel from 10 to 60 degrees θ. (a) Before CO_2 laser irradiation; (b) after CO_2 laser treatment. H: hydroxyapatite, α: α-tricalcium phosphate.

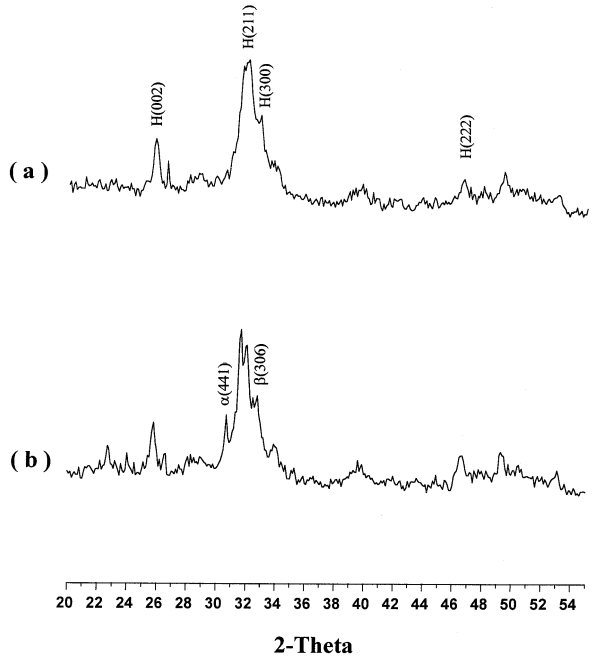

Figure 2 XRD patterns of the dentin from 10 to 60 degrees 2θ. (a) Before CO_2 laser irradiation; (b) after CO_2 laser treatment. H: hydroxyapatite, α: α-tricalcium phosphate, β: β-tricalcium phosphate.

3.2. FTIR analysis

In the FTIR pattern of enamel before CO_2 laser irradiation, the bands at 602 and 568 cm^{-1} (doublet) arose from the ν_4 phosphate mode (Fig. 3a). The band of tooth enamel at 470 cm^{-1} arose from the ν_2 phosphate mode and the shoulder at about 3572 cm^{-1} arose from hydroxide ''translation'' as acknowledged by the comparison with the assigned modes in hydroxyapatite. The bands at 1450, 1410 and 870 cm^{-1} were absorption bands of CO_3^{-2} in biological apatite, which proved that the mineral in enamel is carbonate-containing apatite. The spectra of the laser-irradiated tooth enamel showed that (1) a minor phase of α-TCP appeared as shown by the weak new bands at 502, 475, 440 and the very weak shoulders at $\sim$985 and $\sim$940 cm^{-1}; and (2) the major phase was still hydroxyapatite (hydroxyapatite phosphate bands at $\sim$1090, $\sim$1040, 958, 602, 568 and 470 cm^{-1}); (3) the absorption bands of OH^- (1630 and 630 cm^{-1}) and CO_3^{-2} (1450 and 1410 cm^{-1}) decreased due to dehydration, protein destruction, and carbonate evaporation (Fig. 3b).

In the FTIR pattern of dentin before laser irradiation, the absorption band of OH^- at 1630 cm^{-1} of dentin was obviously higher than that of enamel due to the higher

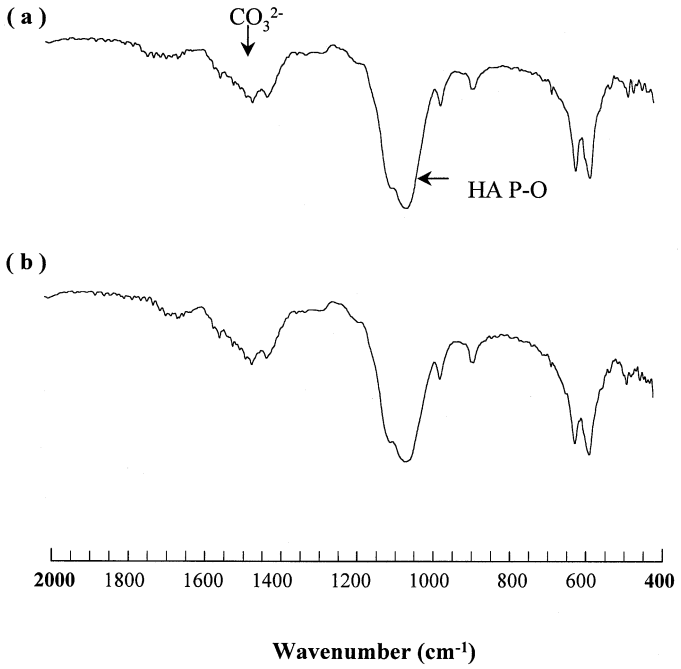

Figure 3 FTIR patterns of the enamel. (a) Before CO_2 laser irradiation; (b) after CO_2 laser treatment.

water content in dentin (Fig. 4a). The strong- and medium-absorption bands at 1040, 1093, 733 and 692 cm^{-1} confirmed the presence of tetrahedral orthophosphate ion PO_4^{-3} in the hydroxyapatite structure. The most intense bands associated with PO_4^{-3} vibration in calcium phosphate were the antisymmetric stretching mode at 1100–1000 cm^{-1} (ν_2 band) and antisymmetric bending mode at 600–550 cm^{-1} (ν_4 band). The band at 1210 cm^{-1} was the absorption band of HO-HPO_4^-, at 1133 cm^{-1} was the vibrating mode of HPO_4^{-2}; at 870 cm^{-1} was the absorption band of P-O-H; and that at 634 cm^{-1} attributed to OH^- vibration. After laser treatment (Fig. 4b), the dentin showed a decrease in the absorption bands of OH^- (1630 and 630 cm^{-1}) and CO_3^{-2} (1450 and 1410 cm^{-1}) due to dehydration, protein destruction and carbonate evaporation, a phenomenon similar to that in laser irradiated enamel.

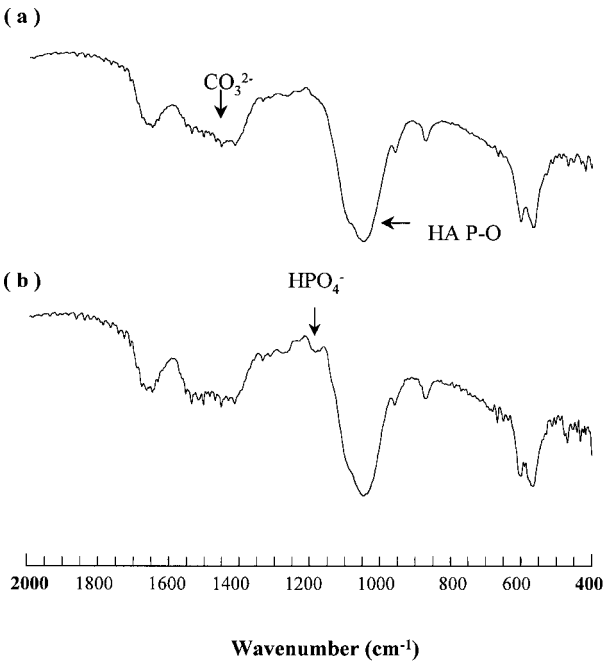

Figure 4 FTIR patterns of the dentin. (a) After CO_2 laser irradiation; (b) before CO_2 laser treatment.

3.3. DTA/TGA

From the results of DTA for tooth enamel before laser irradiation, the endothermic peak at 50–200 °C was due to surface water and organically-bound water evaporation on the enamel (Fig. 5a). The pyrolysis and volatilization of various organic constituents in the enamel occurred in the temperature range of 250–350 °C as illustrated by the continuous and broad exothermic peak [14]. From the results of TGA of the enamel, we could observe weight loss in the two temperature ranges (Fig. 5b). The organic content in dentin (33%) is much higher than that in enamel (4%), which resulted in a larger endothermic peak, exothermic peak (Fig. 6a) and higher weight loss (Fig. 6b) in dentin in the two temperature ranges. The maximum rate of oxidation and volatilization of the organic constituents of both enamel and dentin took place at 350 °C.

The continuous endothermic reaction of both enamel (Fig. 5a) and dentin (Fig. 6a) from 500–900 °C represented the subsequent oxidation of carbon compounds from the inorganic phase. It also reflected on the TGA curves of the enamel (Fig. 5b) and dentin (Fig. 6b). Enamel had an exothermic reaction at 1300–1400 °C, resulted from the thermal decomposition of hydroxyapatite into α-TCP ($Ca_3(PO_4)_2$) and TTCP ($Ca_4P_2O_9$). The exothermic reaction of dentin at the temperature of 1300–1400 °C was more distinct than that of enamel because the differences in particle size and crystal structure. Though both enamel and dentin are identified as hydroxyapatite lattice with XRD, they are different in ionic composition. Enamel is a carbonate-con-

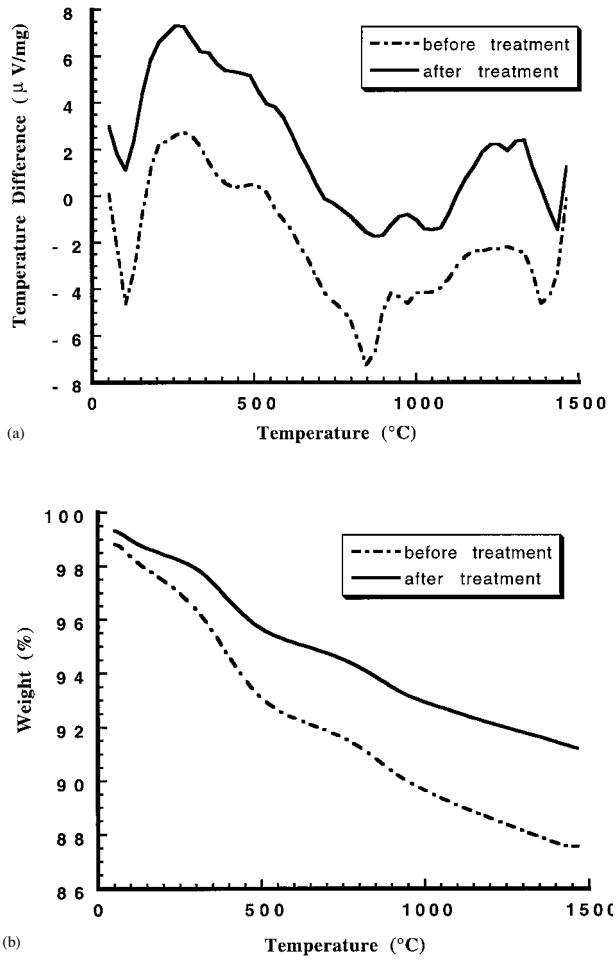

Figure 5 (a) DTA curves of the enamel before (- · - ·) and after (–) laser treatment. (b) TGA curves of the enamel before (- · - ·) and after (–) laser treatment.

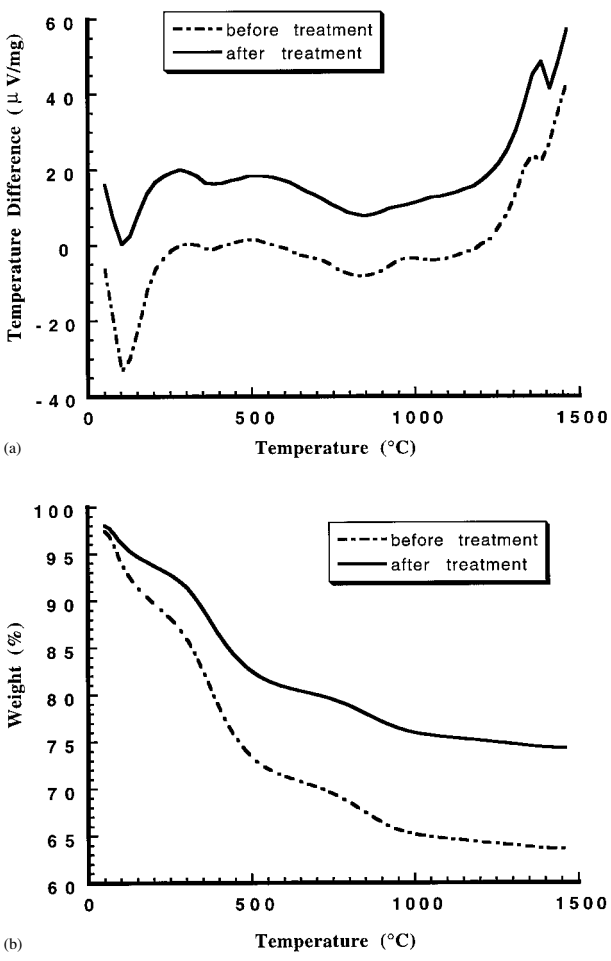

Figure 6 (a) DTA curves of the dentin before (- · - · -) and after (–) laser treatment. (b) TGA curves of the dentin before (- · - · -) and after (–) laser treatment.

taining hydroxyapatite of $Ca_{10-x}(PO_4)_{6-3x/2}(CO_3)_{3x/2}(OH)_{2-x/2}x/2H_2O$ where the CO_3^{-2} ions take the position of PO_4^{-3}. Dentin is a calcium-deficient hydroxyapatite of $Ca_{10-x}(HPO_4)_x(PO_4)_{6-x}(OH)_{2-x}$ $(0<x<2)$ containing HPO_4^{-2} group [15, 16].

Except for the peak at 1300–1400 °C, all other endothermic and exothermic peaks on the DTA curves of both the laser-treated enamel and dentin were much smaller than those on the curves before treatment. This phenomenon resulted from the loss of water and organic constituents in the laser-treated materials. A similar effect was also observed on the TGA curves, reflecting a smaller amount of weight loss during heating after laser treatment.

3.4. Microstructure

Before CO_2 laser irradiation, a regular head and tail arrangement of the enamel prisms was observed under SEM (Fig. 7a). At higher magnification of the prism cores, the prefered three-dimensional orientation of the crystals could be demonstrated (Fig. 7b). After laser treatment, a melted area with small craters formed on the enamel surface by right-angled CO_2 laser beam (Fig. 8a). The thermal gradient generated by laser irradiation resulted in the sintering of hydroxyapatite grains to form larger grains. There were some crazes and cracks on the surface of the enamel, which resulted from rapid water evaporation and organic decomposition during heating by the CO_2 laser. In the center of the melted area, glass-like structure, probably composed of melted hydroxyapatite, was observed in which recrystallization and resolidification of the enamel crystals occurred (Fig. 8b).

Before CO_2 laser irradiation, the sectioned dentin surface was normally covered by a smear layer (Fig. 9a). In some instances, the typical microstructures of dentin including dentinal tubules, peritubular dentin and the collagen network in intertubular dentin were observed under SEM (Fig. 9b). The diameters of the dentinal tubules are about 2–4 μm. After CO_2 laser treatment, surface melting of the dentin occurred, causing a crater to form (Fig. 10a). Inside and around the crater, melting and fusion of dentin was observed. At higher magnification, recrystallization and resolidification of dentin occurred during laser irradiation (Fig. 10b).

4. Discussion

Laser irradiation will generate a temperature gradient on the tooth enamel and dentin. Laser-irradiant conditions of high energy density (10,000 J/cm^2) easily melt and penetrate the enamel and dentin [17]. Even under irradiant conditions of lower energy density (9–120 J/cm^2), slight surface melting has been detected which

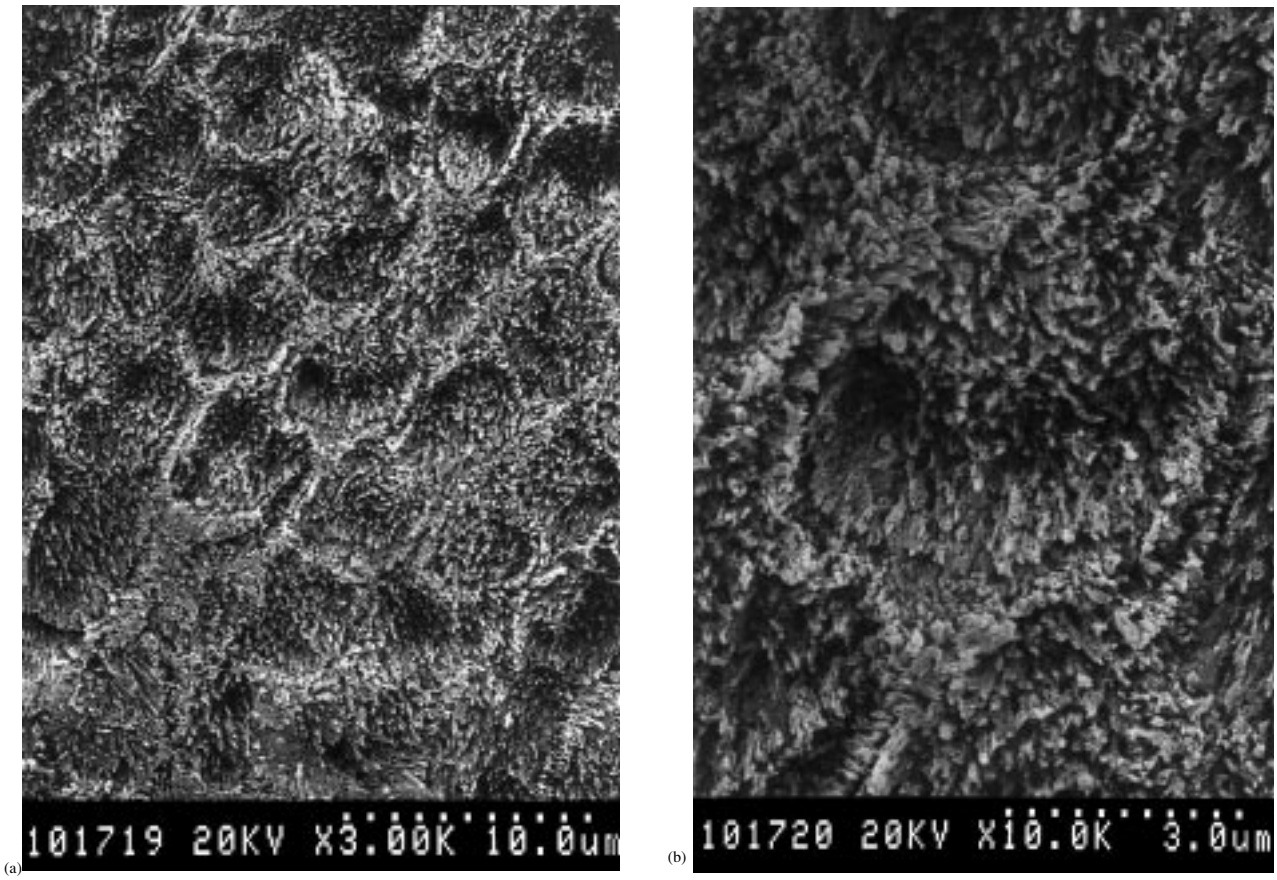

Figure 7 SEM micrographs of the enamel before laser irradiation. (a) A regular head and tail arrangement of the enamel prisms was observed. (b) At higher magnification of the prism cores, the preferred three-dimensional orientation of the crystals could be demonstrated.

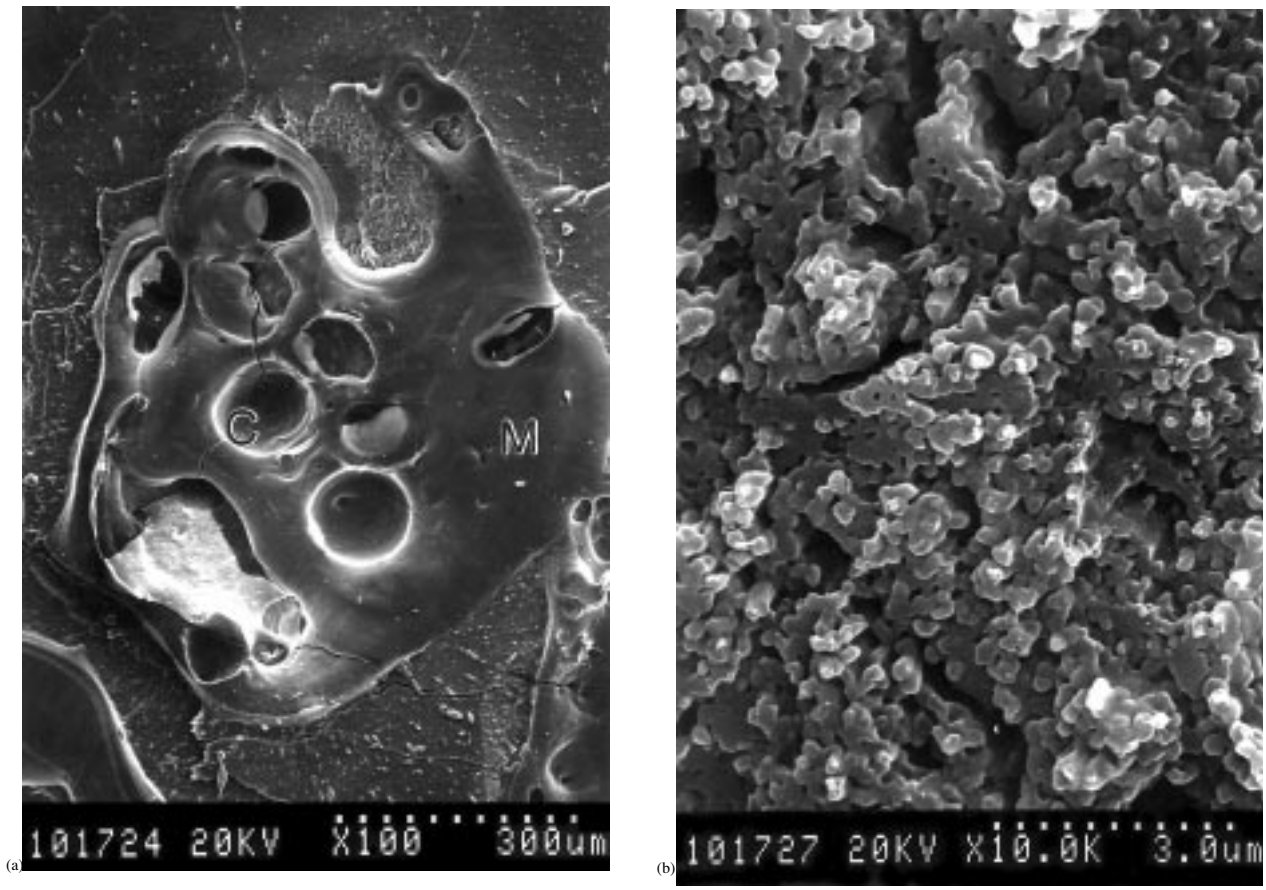

Figure 8 SEM micrographs of the enamel after laser treatment. (a) A melted area with small craters formed on the enamel surface by right-angled CO_2 laser beam. Cracking and crazing caused by local heating during laser irradiation was noted. C: crater; M: melted enamel. (b) In the center of the melted area, a glass-like structure probably composed of melted hydroxyapatite, was observed in which recrystallization and resolidification of the enamel crystals occurred.

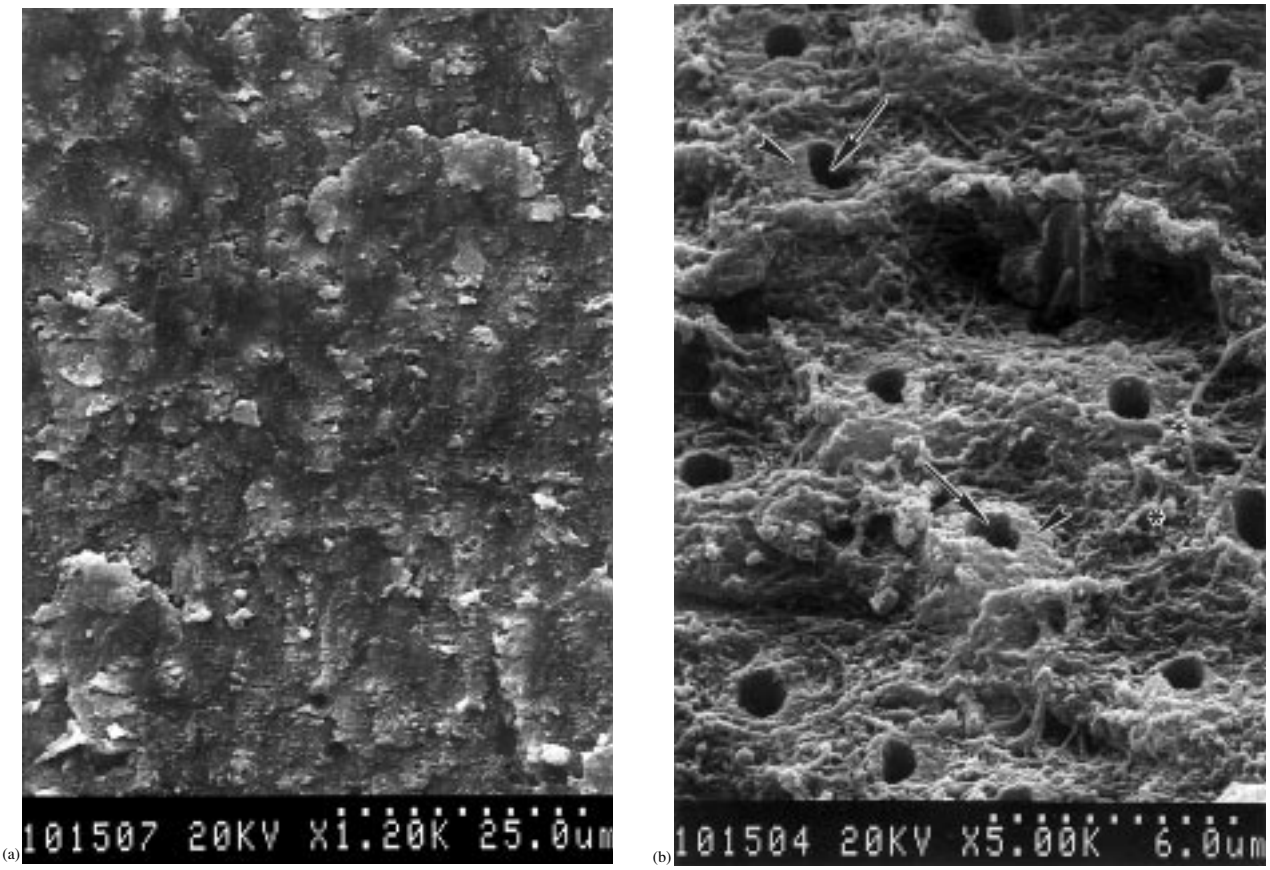

(a) (b)

Figure 9 SEM micrographs of the dentin before laser irradiation. (a) A smear layer normally covered the sectioned dentin surface. (b) In some instances, the typical microstructures of dentin including dentinal tubules (arrows), peritubular dentin (arrowheads) and the collagen network in intertubular dentin (asterisks) were demonstrated. The diameters of the dentinal tubules are about 2–4 μm.

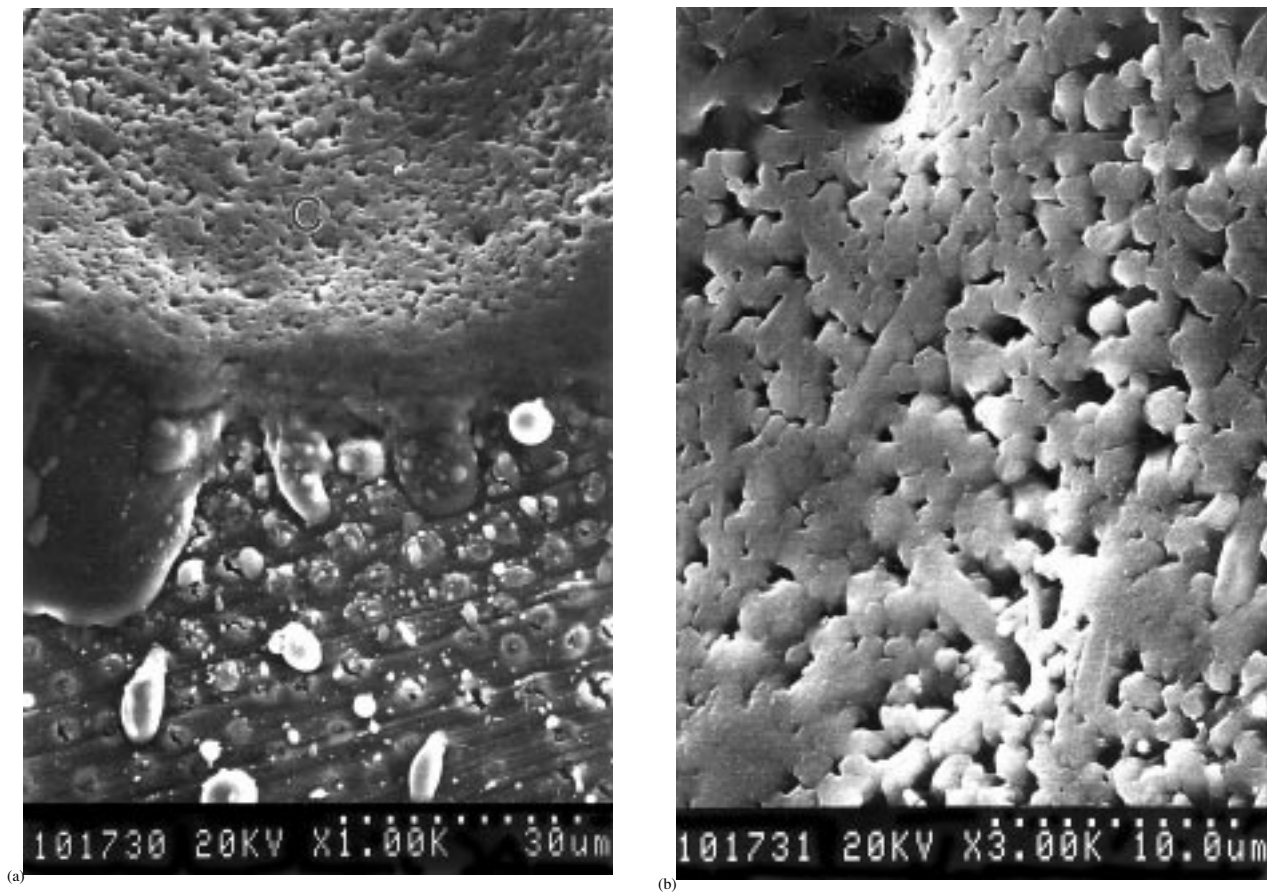

(a) (b)

Figure 10 SEM micrographs of the dentin after laser treatment. (a) Surface melting of the dentin occurred, causing a crater to form. C: crater. (b) At higher magnification, recrystallization and resolidification of dentin was observed inside and around the crater.

indicates very high temperatures occurred at the enamel and dentin surface [12, 18, 19]. Along the temperature gradient, different compositional, structural and phase changes are expected.

The effect of lasers on dental hard tissues is caused mainly by the changes in temperature that can be extremely high at the irradiated spot even for a short action time. Consequently, the hard tissues melt, vaporize and a crater is formed at the irradiation site. Laser energy causes a quick local temperature rise and prompts melting and cooling of the apatite crystals. Heat conduction should lead to a thermal equalization between the pronouncedly heated components and the surrounding tissues with a laser pulse in the order of a few microseconds. Since the changes in laser irradiated enamel and dentin are considered mainly due to the localized heating, the alterations are expected to be similar to those occurring in the biological hydroxyapatite progressively heated in a conventional furnace.

When the biological hydroxyapatite is heated in a conventional furnace, the thermal changes could be divided according to three temperature ranges [14, 16–18]: I, 100–650 °C; II, 650–1100 °C; and III, > 1100 °C. The following changes occur in temperature range I (100–650 °C): (1) The water content decreases, most abruptly at 100–300 °C in which about 1/3 of the total water content is lost. (2) An overall reduction in total CO_3^{-2} content and rearrangement of $CO_3{}^{-2}$ ions occur; the amount of CO_3^{-2} in ''phosphate'' position progressively decreases at 400–650 °C. (3) The OH^- content progressively increases to a maximum of $\sim$1.8 times of the original in the 300–500 °C range. (4) Acid phosphate (HPO_4^{-2}) ions condense to form pyrophosphate ($P_2O_7^{-4}$) ions. (5) Progressive uptake of CO_2 and NCO^- occur in the range of 500–600 °C, and then both ions decrease with increasing temperature. (6) Proteins decompose at about 250–600 °C.

In this study, the results of DTA/TGA of enamel and dentin (Figs 5 and 6) in the temperature range I largely followed the previous description. Water content decreased around 100–300 °C and proteins decomposed at about 250–600 °C. There was a ''saddle'' on the TGA curves of dentin and enamel at the temperature of 500–800 °C, which meant no weight loss in this range. Although organic constituents gradually decomposed, progressive uptake of some ions such as CO_2, NCO^-, and OH^- occurred in this temperature range, therefore resulted in a dynamic balance of weight in the system. In the FTIR analysis, an HPO_4^{-2} absorption band could be traced in the dentin without laser treatment. However, it disappeared after the dentin was exposed to laser. As noted above, HPO_4^{-2} ions condensed into pyrophosphate ($P_2O_7^{-4}$) ions at the temperature of 500–600 °C and that made the decrease of HPO_4^{-2} band [17, 18, 20] Hydroxyapatite of the enamel contains no HPO_4^{-2} ions in the crystal structure. Therefore, there was no significant change in the absorption band of HPO_4^{-2} on the FTIR curves of enamel before and after laser treatment.

The thermal changes in temperature range II (650–1100 °C) are as follows: (1) Thermal recrystallization and growth of crystal size occur. Pyrophosphate reacts with apatite to form PO_4^{-3} at $\sim$650 °C or lower, along with the formation of a second phase of β-TCP. The beta-form of TCP normally converts to the alpha-form at 1125 °C. (2) The OH^- content changes from $\sim$1.8 times of the original to $\sim$1.4 times of the original at 600–650 °C. (3) Additional water and CO_3^{-2} are lost from the apatite. (4) All trapped CO_2 and NCO^- are lost by 800 °C.

In this study, the slope in the range of 500–800 °C on the TGA curves of both the enamel and dentin resulted from the loss of water, OH^-, trapped CO_2 and NCO^-. Growth in grain size was expected at temperatures up to 650 °C. Enamel is a pure carbonate-containing hydroxyapatite, and there will be no obvious phase transformation if the heating temperature is below 1400 °C. Dentin is a nonstoichiometric hydroxyapatite: $Ca_{10-x}(HPO_4)_x(PO_4)_{6-x}(OH)_{2-x}(0<x<2)$ and a series of reactions will happen as the temperature increases [14, 16, 19]:

$$2HPO_4{}^{-2} \Rightarrow P_2O_7{}^{-4} + H_2O \qquad (250\text{–}550°C) \quad (1)$$

$$P_2O_7^{-4} + 2OH^- \Rightarrow 2PO_4{}^{-3} + H_2O \qquad (600\text{–}700°C) \quad (2)$$

From the reaction, β-TCP will be formed in dentin once the temperature is higher than 700 °C. Dentin treated with CO_2 laser showed β-TCP peaks at the position of $2\theta = 32.47$ and 33.05° (Fig. 2) but enamel had no β-TCP formed after laser irradiation.

The thermal changes in temperature range III are as follows (over 1100 °C): (1) The β-TCP converts to α-TCP at 1125 °C and α-TCP converts at 1430 °C to a higher temperature polymer designated as $\underline{\alpha}$-TCP which melts at 1756 °C. (2) The remaining CO_3^{-2} and Cl^- are lost along with further OH^- reduction and concomitant O^{-2} incorporation into the apatite phase. The oxyhydroxyapatite phase decomposes at 1450 °C to form $\underline{\alpha}$-TCP and TTCP and the mixture melts at 1600 °C.

In this study, α-TCP could be traced on the XRD curves of enamel and dentin after laser treatment but no $\underline{\alpha}$-TCP appeared. Though α-TCP converts at 1430 °C to a higher temperature polymer designated as $\underline{\alpha}$-TCP; the $\underline{\alpha}$ form is not stable at room temperature. Glass-like and melted structures could be observed in the SEM photographs of the enamel and dentin after laser irradiation. We speculate that the temperature on the surface of enamel and dentin during the irradiation should be over 1600 °C.

Warshawsky [21] has shown that the hydroxyapatite orientation is almost parallel to the *c*-axis in the surface part of enamel. It is tilted by about 40° and 60° to the c-axis of the rhombohedral prism in the middle and inner parts of the enamel. Therefore, the crystal orientation of the enamel from outer to inner is like a fan-out fashion along the rhombohedral prism. The (0 0 2) plane of the hydroxyapatite prism parallels to the surface of enamel resulting in the higher hardness in this plane. The (4 1 2) and (1 1 2) directions of the prisms parallel to the (0 0 2) direction cross over each other and contribute to the high mechanical strength of the enamel. From the results of the present study, there were no significant differences in the XRD pattern of enamel after CO_2 laser treatment, as compared with that before laser treatment. However,

there was a small peak belonging to α-TCP at the position of $2\theta = 30.78^\circ$.

The results of this study indicate that the morphological changes in the surface structures of enamel and dentin vary with different energy levels applied by laser irradiation. Melting and resolidification may occur in both enamel and dentin by medium energy CO_2 laser. This implies that using a continuous-wave CO_2 laser of medium energy density to fuse a low melting-point bioactive glass to the enamel/dentin is possible.

In conclusion, after exposure to CO_2 laser, there was no significant difference in XRD patterns of enamel when compared to that before treatment. However, a small peak belonging to α-TCP appeared at the position of $2\theta = 30.78^\circ$. After irradiation, the dentin showed much sharper peaks in XRD patterns because of grain growth and better crystallinity. Four peaks other than hydroxyapatite could be traced at the positions of $2\theta = 30.78^\circ/34.21^\circ$ and $32.47^\circ/33.05^\circ$ in the diffraction patterns which were identified to be α-TCP and β-TCP, respectively. In the FTIR analysis, a HPO_4^{-2} absorption band could be traced in the dentin before laser treatment and it disappeared after the exposure to laser because of the condensation of HPO_4^{-2} into $P_2O_7^{-4}$. Hydroxyapatite of the enamel contains no HPO_4^{-2} in the crystal structure which resulted in no significant change in the absorption band of HPO_4^{-2} before and after laser treatment. Under the SEM, melting and resolidification occurred in both enamel and dentin by medium energy CO_2 laser. This implies that using a continuous-wave CO_2 laser of medium energy density to fuse a low melting-point bioactive glass to the enamel/dentin is possible. We believe these phase changes and thermal data can make a useful guide for future studies on the thermal interaction and bridging mechanism between the bioactive glass and enamel/dentin under CO_2 laser irradiation.

References

1. J. O. ANDREASEN, in ''Traumatic injury of the teeth'', (Mosby, St. Louis, MO, 1981) p. 15.
2. M. ABOU-RASS, *Oral Hygiene* **4** (1983) 437.
3. E. BASRANI, in ''Fractures of the teeth: prevention and treatment of the vital and non-viral pulp'', (Lea & Febige, Philadelphia, PA, 1985) p. 43.
4. D. L. PITTS and E. NATKIN, *J. Endodon.* **9** (1983) 338.
5. G. G. STEWART, *ibid.* **14** (1988) 47.
6. S. FRIEDMAN, M. MOSHONOV and M. TROPE, *Endod. Dent. Traumatol.* **9** (1993) 101.
7. L. STEWART, G. L. POWELL and S. WRIGHT, *Oper. Dent.* **10** (1985) 2.
8. G. C. LEVY and G. F. KOUBI, *Compend. Contin. Educ. Dent.* **16** (1993) 144.
9. S. ARAKAWA, W. J. KILLOY and P. SPENCER, *J. Endodon.* **22** (1996) 662.
10. G. C. LEVY, *ibid.* **18** (1992) 123.
11. H. A. WIGDOR, J. T. WALSH, J. D. B. FEATHERSTONE, S. R. VISURI, D. FRIED and J. L. WALDVOGEL. *Lasers Surg. Med.* **16** (1995) 103.
12. Y. KIMURA, P. WILDER-SMITH, A. M. A. ARRASTIA-JITOSHO, L. H. L. LIAW, K. MATSUMOTO and M. W. BERNS, *ibid.* **20** (1997) 15.
13. T. F. ANDERSON, *Trans NY Acad. Sci.* **13** (1951) 130.
14. B. LOCARDI, U. E. PAZZAGLIA, C. GABBI and B. PROFILO, *Biomaterials* **14** (1993) 437.
15. R. M. BLITZ and E. D. PELLERGRINO, *J. Dent. Res.* **62** (1983) 1190.
16. F. H. LIN, C. J. LIAO, K. S. CHEN and J. S. SUN, *Biomaterials* **19** (1998) 1101.
17. S. KURODA and B. O. FOWLER, *Calcif. Tissue Int.* **36** (1984) 361.
18. J. T. GORGIA and W. E. MOODY, *J. Dent. Res.* **53** (1974) 571.
19. J. H. KINNEY, D. L. HAUPT, M. BALOOCH, J. M. WHITE, W. L. BELL, S. J. MARSHALL and G. W. MARSHALL, *ibid.* **75** (1996) 1388.
20. L. LAUNAY, S. MORDON, A. CORNIL, J. M. BRUNETAUD and Y. MOSCHETTO, *Lasers Surg. Med.* **7** (1987) 473.
21. H. WARSHAWSKY, *Anatomical Record* **224** (1989) 242.

Received 9 September 1998
and accepted 16 September 1999